The temperature dependence of resistivity and thermoelectric power in lanthanum molybdenum oxide crystal $La_2Mo_2O_7$

1996 J. Phys.: Condens. Matter 8 3413

(http://iopscience.iop.org/0953-8984/8/19/016)

J. Phys.: Condens. Matter **8** (1996) 3413–3418. Printed in the UK

The temperature dependence of resistivity and thermoelectric power in lanthanum molybdenum oxide crystal $La_2Mo_2O_7$

Tian Mingliang, Mao Zhiqiang and Zhang Yuheng

Structure Research Laboratory, University of Science and Technology of China, Hefei 230026, Anhui, People's Republic of China, and Centre for Advanced Studies in Science and Technology of Microstructures (CASSTM), Nanjing 210093, People's Republic of China

Received 19 December 1995, in final form 5 February 1996

Abstract. Electrical resistivity, voltage–current (V–I) characteristics and thermoelectric power (TEP) at various temperatures in the quasi-two-dimensional single crystal $La_2Mo_2O_7$ were measured. It was found that at 130 K the resistivity shows a metal–semiconductor transition, and the TEP has a minimum value. In the semiconducting states below 130 K, the electronic transport presents a clear non-linear behaviour. By analysis of the above data, it is indicated that above 130 K the crystal is a metal and electrons are dominant carriers; below 130 K the crystal becomes a semiconductor with a small energy gap, the two types of carrier being possibly co-existent. The anomalies of TEP and resistivity near 130 K may be associated with the formation of so-called charge-density waves due to the partial opening of a gap.

1. Introduction

The electronic and structural properties of transition metal oxide crystals have received much attention, and among them, in particular, the reduced ternary molybdenum oxides are of great interest. For instance, the monovalent alkali metal molybdenum bronzes A_xMoO_{3+y} [1–3], which are non-stoichiometric compounds, exhibit a wealth of structural complexity with concentration x and a variety of physical phenomena with a charge-density wave (CDW) driven structural phase transition [2, 4, 5] and superconductivity [6]. Besides, the divalent cation (Ba, Sr or Ca) molybdenum oxides [7, 8] with well characterized perovskite type structure, and the trivalent cation (Bi, Sb) molybdenum oxides [9, 10] have also been synthesized and have been extensively studied.

Another interesting class with variable notable features of chemistry and physical properties, ternary rare earth molybdenum oxides, have also attracted much attention recently. $R_2Mo_2O_7$ is one of these rare earth molybdenum compounds, for R = Sm–Lu or Y; the structures characterized by x-ray powder diffraction have shown to be of the pyrochlore type [11], and the polycrystalline samples can be prepared by solid state reactions. Further, they are all low-resistivity, n-type semiconductors with activation energies in the 5–20 meV range. In contrast, $La_2Mo_2O_7$ [12, 13] was considered to be a new type of compound having similar formula, but having distinctly different structures and the physical properties from the pyrochlore-type $R_2Mo_2O_7$ (R = Sm, Lu and Y etc) series, and the single crystals can be prepared by the fused salt electrolytic method [13]. The structure can be considered to be two dimensional with respect to the Mo–O network, and the infinite two-dimensional

0953-8984/96/193413+06$19.50

Mo–O layers parallel to the *ac* plane of the orthorhombic unit cell and the MoO_6 octahedra are linked by sharing corners in the *ac* plane. These structural features are different from the $R_2Mo_2O_7$ (R = Sm, Lu, Y) series, in which the Mo–O network forms a complex three-dimensional structure. In addition, the transport properties of $La_2Mo_2O_7$ crystals [12] are also interesting: an anomaly of resistivity near 130 K has been found, and is considered to be related to a possible second-order phase transition, which is likely to be associated with the onset of a charge-density wave since this type of transition is often related to quasi-one- or quasi-two-dimensional materials, where the Fermi surface is entirely or partially overlapped with the Brillouin zone at T_p due to Peierls instabilities.

However, up to now, detailed studies on the transport properties and the phase transition are lacking; relatively little is known about the electronic structure. In this paper, we investigate the resistivity, V–I responses and thermoelectric power (TEP) properties, and provide new evidence for the phase transition near 130 K which is associated with CDW instabilities.

2. Experimental preparation

Single crystals of $La_2Mo_2O_7$ used in this work were grown at 1130 °C by electrolysis of the melt made from a mixture of $Na_2MoO_4 \cdot 2H_2O$, MoO_3 and La_2O_3 in a molar ratio of 2.4:2.4:1.0. The mixture of stoichiometric quantities was carried out in an alumina crucible in steps at 800, 1000, 1100 and 1130 °C for 48 h each, then keeping it at 1130 °C for electrolysis. A Pt slice with a size of $10 \times 10 \times 0.5$ mm^3 and a Pt wire with a diameter of $\phi \approx 0.8$ mm were, respectively, used for the anode and the cathode; the dc current for electrolysis is 100 mA. The crystals grew out from the cathode in the form of purple-brown needles with a size of approximately $0.3 \times 0.3 \times 3$–10 mm^3. The structures were characterized by the x-ray diffraction method: the parameters of unit cell are about $a = 12.212$ Å, $b = 6.040$ Å, $c = 3.854$ Å and $\alpha = \beta = \gamma 90°$, in good agreement with those reported by Moini *et al* [12] and McCarroll *et al* [13].

The electrical resistivity and the V–I characteristics were measured by the normal four-probe configuration along the *c* axis (needle direction). The electric contacts were made by evaporating an Au film; Au wires were attached to the Au-film areas by Ag paint. The single-crystal size used in this measurement is about $0.3 \times 0.2 \times 3$ mm^3, the distance between the two voltage contacts is about 0.5 mm. The sample was mounted in the vacuum chamber of a refrigerator, and the temperature could be changed in the range of 10–300 K. TEP measurements were carried out quasi-statically by use of the conventional differential method in the liquid nitrogen range [14]. The temperature gradient along the *c* axis of the crystal was measured by means of two Rh–Fe resistance thermometers. The voltage between the two ends of sample was measured by a Keithley 181 nanovoltmeter; the system was carefully calibrated by the use of high-purity Pb before carrying out our TEP measurements for the crystal.

3. Results

Figure 1 shows the temperature dependence of the electrical resistivity, ρ, of the $La_2Mo_2O_7$ single crystal in the range of 10–300 K; the inset is the enlarged portion of the curve above 170 K. It is seen that the resistivity ρ has a positive slope above 174 K with a small magnitude of the order of 10^{-2} Ω cm, while below about 130 K the resistivity exhibits a steep increase with decreasing T. This indicates that the compound displays a metallic

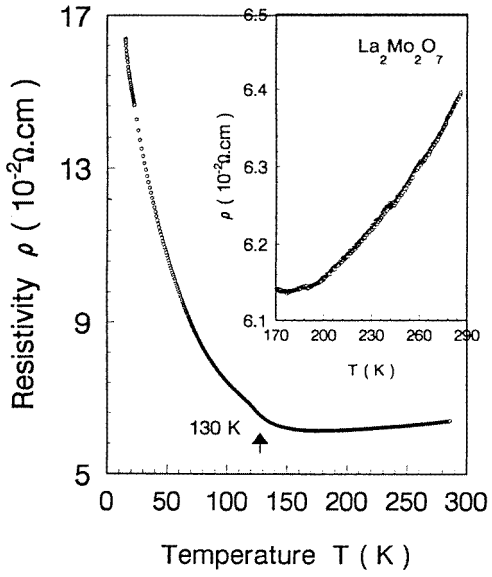

Figure 1. Electric resistivity ρ versus temperature T in the range of 10–300 K for single-crystal $La_2Mo_2O_7$; the inset is the enlarged portion of the curve above 170 K.

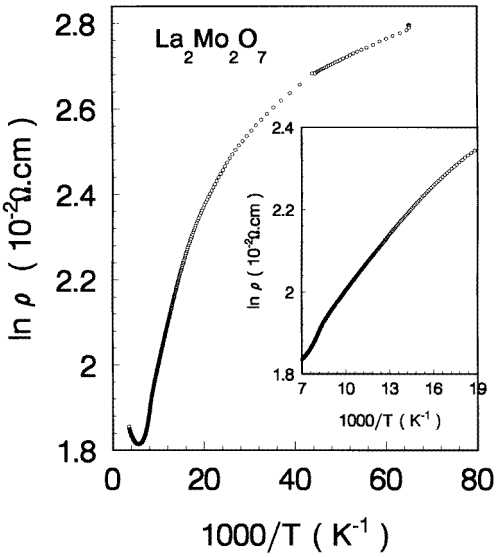

Figure 2. Electric resistivity ρ in a logarithmic scale against reciprocal temperature T in the range of 10–300 K; the inset shows the enlarged part of the curve in the range of 140–50 K. The data approximately fit the thermal activated form, $\rho \propto e^{\Delta/k_B T}$, $\Delta \sim 4$ meV, in the range of 110–70 K.

behaviour at higher temperatures, and below 130 K presents semiconducting properties. These phenomena are qualitatively in agreement with those reported by Moini *et al* [12]. From figure 1 another anomaly near 60 K observed by Moini *et al* [12] was not found in

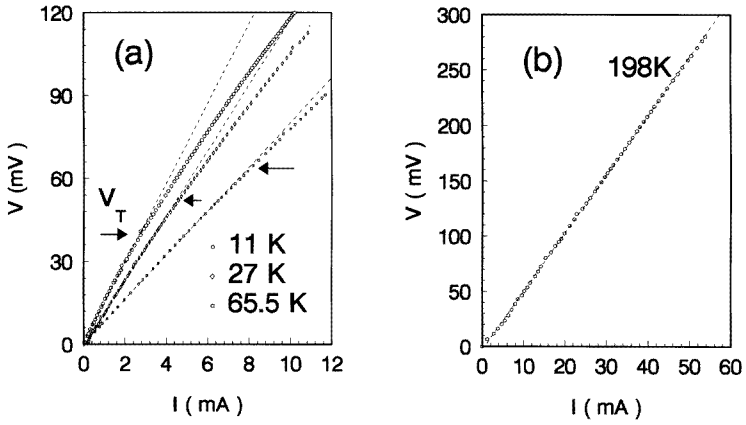

Figure 3. Voltage–current (V–I) characteristics at several temperatures: (a) 11, 27 and 65.5 K; (b) 198 K. The arrows show the threshold voltage V_t, above which the V–I response deviates from linearity.

our measurements.

Figure 2 shows a plot of $\ln \rho$ versus reciprocal temperature T; the inset is the enlarged part of the curve below about 140 K. Obviously, the curve does not fit a simple linear relation in the entire temperature range below 130 K, but in the very much shorter temperature range 110–70 K the data can be approximately described by the simple thermal activation law, $\rho \sim \mathrm{e}^{E_g/2k_BT}$, where E_g is the thermal activation energy gap and k_B is the Boltzmann constant. This gives $E_g \approx 8.0$ meV.

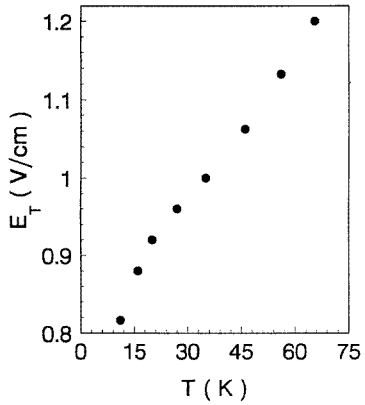

Figure 4. Threshold electric field E_t versus temperature T in the range of 10–75 K.

Figure 3 shows several typical voltage–current (V–I) characteristics at various temperatures. It is seen that below 130 K non-linear transport behaviour is clearly observed when the electric field exceeds a critical voltage V_t. With increasing temperatures, the non-linear properties of V–I responses are gradually weakened. Above 130 K, the non-linear feature disappears completely. If we define this critical voltage value V_t which deviates from linearity, shown by the arrows, in terms of the threshold electric field $E_t = V_t/d$ (d is the distance between the two voltage contacts), the temperature dependence of E_t is given as shown in figure 4. It is found that E_t increases monotonically with increasing T,

and the magnitude is of the order of 0.8–1.2 V cm^{-1}. Such non-linear properties and the order of magnitude of the threshold are very similar to those in quasi-one-dimensional blue bronze [15], where the non-linear transport is attributed to the motion of charge-density waves depinned from impurities.

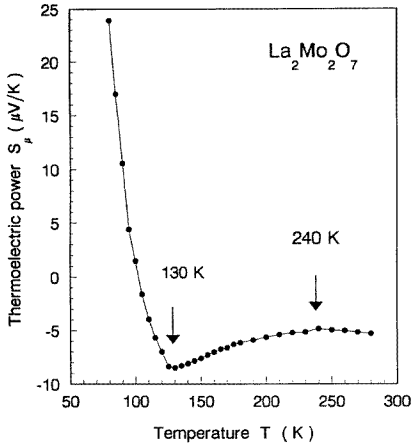

Figure 5. TEP S_μ versus temperature T in the range of 80–280 K.

Figure 5 shows the temperature dependence of the TEP in the range of 80–280 K. It is seen clearly that, above 130 K, the sign of the TEP is negative and the absolute values, $|S_\mu|$, decrease gradually with increasing temperatures; when the temperature reaches about 240 K, $|S_\mu|$ begins to increase slightly with increasing T. In the range of 102–130 K, TEP is still negative, but the absolute values, $|S_\mu|$, decrease rapidly with decreasing T; when $T < 102$ K, TEP changes sign and becomes positive; the magnitude increases steeply with falling temperature and reaches about 25 μV K^{-1} at 80 K. Near 130 K, the TEP shows a clear minimum value; this anomaly is in good agreement with the measurement of resistivity.

4. Discussion

From the measurements of resistivity and TEP shown above, the compound is metallic above 130 K (electrons would be the dominant carriers for the transport), while below 130 K it becomes a semiconductor with a small thermal activated energy gap, 8 meV, and in the TEP a sign change from negative to positive takes place at about 102 K; this implies that both types of carrier, electrons (e) and holes (h), would be co-existent below 130 K (the sign of the TEP would be determined by the competition between the two carriers contributing TEP). Thus, the total TEP should be ascribed to the form of the Nordheim–Gorter rule [16], $S_\mu = (\sigma_h/\sigma)S_h + (\sigma_e/\sigma)S_e$, where $\sigma = \sigma_h + \sigma_e$ is the total conductivity, and $\sigma_h(\sigma_e)$ denotes the hole (electron) conductivity. The occurrence of the holes below 130 K is closely related to the properties of the Fermi surface of the crystals; the anomalous behaviour of TEP near 130 K is quite similar to that in quasi-two-dimensional purple bronze $K_{0.9}Mo_6O_{17}$ [9], where below the transition temperature 120 K the TEP becomes positive due to a partial opening of a gap at the Fermi surface, while above 120 K the TEP becomes negative due to the disappearance of the gap. Hence, in such a $La_2Mo_2O_7$ compound with two-dimensional structures, similar anomalous behaviour for TEP near 130 K may also result from a possible thermodynamic phase transition, which is associated with the instabilities of a charge-density wave. Above 130 K, the features of the Fermi surface should be dominated

mainly by electrons due to the disappearance of the gap; at $T < 130$ K, the phase transition is very likely to be due to a partial opening of a small gap at the Fermi surface, which leads to a change in the concentration of both types of carriers, electrons and holes.

Direct evidence to support the above speculation is further confirmed by the measurements of $V–I$ characteristics, where, in the low-temperature regime below 130 K, a clear non-linear transport behaviour is observed; when the field is larger than a critical value V_t, the conductivity increases with increasing applied field; these phenomena are in good agreement with the model of the sliding motion of charge-density wave depinning in the presence of an applied electric field larger than a critical value V_t. In the normal metallic states above 130 K, the non-linear behaviour was not observe in quite a wide field range.

In addition, it has also to be noted that the temperature dependence of the resistivity shown in figure 2 deviates clearly from linearity below about 70 K, indicating that the compound is not an intrinsic semiconductor, and that impurities or other scattering mechanisms may not be neglected at low temperatures. In the range of 130–175 K, the resistivity shows a small negative slope and the absolute TEP also exhibits a meaningful change for decreasing T; these unusual changes might be associated with the complexity of the band structures for this rare earth molybdenum oxide.

In summary, the electronic resistivity, TEP and $V–I$ responses at various temperatures in lanthanum molybdenum oxide $La_2Mo_2O_7$ have been measured in detail. The anomalies of TEP and resistivity near 130 K can be associated with the formation of so-called charge-density waves due to the partial opening of a gap, but, to date, structural evidence due to the modulation of the lattice is still lacking; further studies need to be done and are in progress.

Acknowledgments

This research was supported by the National Foundation of the Natural Science of China and by the Structure Research Laboratory, University of Science and Technology of China.

References

[1] Schlenker C 1989 *Low Dimensional Properties of Molybdenum Bronzes and Oxides* ed C Schlenker (Deventer: Kluwer) p 87
[2] Dumas J and Schlenker C 1993 *Int. J. Mod. Phys.* B **7** 4045
[3] Schlenker C, Dumas J, Escribe-Filippin C, Marcus J and Fourcaudot G 1985 *Phil. Mag.* B **52** 643
[4] Dumas J, Schlenker C, Marcus J and Buder R 1983 *Phys. Rev. Lett.* **50** 757
[5] Pouget J P, Kagoshima S, Schlenker C and Marcus J 1983 *J. Physique Lett.* **44** L113
[6] Matsuda Y, Sato M, Onoda M and Nakao K 1986 *J. Phys. C: Solid State Phys.* **19** 19
Sato M, Matsuda Y and Fukuyama H 1987 *J. Phys. C: Solid State Phys.* **20** L137
[7] Ellerbec L D, Shanks H R, Sidles P H and Danielson G 1961 *J. Chem. Phys.* **38** 298
Sidles P H and Danielson G 1963 *Adv. Chem.* **30** 237
[8] Stanley R K, Morris R C and Moulton W G 1979 *Phys. Rev.* B **20** 5; *Phys. Rev.* B **20** 1903
[9] Schneemeyer L F, Spengler S E, DiSalvo F J and Waszczak J V 1984 *Mater. Res. Bull.* **19** 525
[10] Bonnet A, Conan A, Queinnec H, Ganne M and Dion M 1984 *Phys. Rev.* B **30** 688
Conan A, Bonnet A, Ganne M and Dion M 1985 *J. Phys. Chem. Solids* **46** 721
[11] Hubert P H 1974 *Bull. Soc. Chim. Fr. (France)* 2385; 1975 *Bull. Soc. Chim. Fr. (France)* 475; 1975 *Bull. Soc. Chim. Fr. (France)* 2463
[12] Moini A, Subramanian M A, Clearfield A, DiSalvo F J and McCarroll W H 1987 *J. Solid State Chem.* **66** 136
[13] McCarroll W H, Darling C and Jakubicki G 1983 *J. Solid State Chem.* **48** 189
[14] Ruan Y Z, Wang R P, Huang W and Li Q 1988 *J. Low Temp. Phys.* **10** 47 (in Chinese)
[15] Fleming R M, Schneemeyer L F and Moncton D E 1985 *Phys. Rev.* B **31** 899
[16] Dugdale J S 1977 *The Electrical Properties of Metals and Alloys* ed B R Coles (London: Arnold) p 172